JAERI-Research
98-033

NUMERICAL SIMULATION OF RUNAWAY ELECTRON EFFECT ON PLASMA FACING COMPONENTS

July 1998

Koichiro EZATO, Satoshi SUZUKI, Tomoaki KUNUGI*
and Masato AKIBA

日本原子力研究所
Japan Atomic Energy Research Institute

本レポートは，日本原子力研究所が不定期に公刊している研究報告書です。
入手の問合わせは，日本原子力研究所研究情報部研究情報課（〒319-1195　茨城県那珂郡東海村）あて，お申し越しください。なお，このほかに財団法人原子力弘済会資料センター（〒319-1195　茨城県那珂郡東海村日本原子力研究所内）で複写による実費頒布をおこなっております。

This report is issued irregularly.
Inquiries about availability of the reports should be addressed to Research Information Division, Department of Intellectual Resources, Japan Atomic Energy Research Institute, Tokai-mura, Naka-gun, Ibaraki-ken, 319-1195, Japan.

編集兼発行　　日本原子力研究所

JAERI-Research 98-033

Numerical Simulation of Runaway Electron Effect on Plasma Facing Components

Koichiro EZATO, Satoshi SUZUKI, Tomoaki KUNUGI* and Masato AKIBA

Department of Fusion Engineering Research
Naka Fusion Research Establishment
Japan Atomic Energy Research Institute
Naka-machi, Naka-gun, Ibaraki-ken

(Received June 4, 1998)

The runaway electron effects on Plasma Facing Components (PFCs) are studied by the numerical analyses. The present study is the first investigation of time-dependent thermal response of PFCs caused by runaway electron impact. For this purpose, we developed a new integrated numerical code, which consists of the Monte Carlo code for the coupled electrons and photons transport analysis and the finite element code for the thermo-mechanical analysis. In this code, we apply the practical incident parameters and distribution of runaway electrons recently proposed by S. Putvinski, which can express the time-dependent behavior of runaway electrons impact. The incident parameters of electrons in this study are the energy density ranging from 10 to 75 MJ/m^2, the average electrons' energy of 12.5 MeV, the incident angle of 0.01 deg and the characteristic time constant for decay of runaway electrons event of 0.15sec. The numerical results showed that the divertor with CFC (Carbon-Fiber-Composite) armor did not suffer serious damage. On the other hand, maximum temperatures at the surface of the divertor with tungsten armor and the first wall with beryllium armor exceed the melting point in case of the incident energy density of 20 and 50 MJ/m^2. Within the range of the incident condition of runaway electrons, the cooling pipe of each PFCs can be prevented from the melting or burn-out caused by runaway electrons impact, which is one of the possible consequences of runaway electrons event so far.

Keywords: Runaway Electrons, Plasma Facing Components, Numerical Simulation, ITER

---

* Tokai University

プラズマ対向機器が受ける逃走電子入射による影響に関する数値解析

日本原子力研究所那珂研究所核融合工学部
江里幸一郎・鈴木　哲・功刀　資彰*・秋場　真人

(1998年6月4日受理)

逃走電子入射によりプラズマ対向機器（ＰＦＣ）が受ける影響を解析的に評価した。本研究では、物質内の電子・光子輸送を取り扱うモンテカルロ法と熱解析を行う有限要素法からなる解析コード群を開発し、従来取り扱えなかった逃走電子入射時のＰＦＣ内の非定常温度解析を可能にした。この解析コードには、逃走電子入射の時間変化を考慮した入射条件が組み込まれている。本研究では入射条件として、入射エネルギー密度10－75 MJ/m^2、逃走電子の平均エネルギー12.5 MeV、入射角0.01度、逃走電子入射における減衰の代表時間0.15秒を用いた。ＣＦＣ（炭素繊維強化複合材料）アーマを持つダイバータ表面における逃走電子入射による損傷は発生しないと考えられるが、タングステンアーマを持つダイバータおよびベリリウムアーマを持つ第一壁ではそれぞれ、20、50 MJ/m^{2}程度の入射エネルギー密度で表面が溶融する可能性が本解析により示された。しかしながら、これらの逃走電子入射条件下では、従来懸念されていた熱シンクの溶融や冷却管のバーンアウトが発生しないと考えられる。

那珂研究所：〒311－0193　茨城県那珂郡那珂町向山801－1
＊　東海大学

Contents

目　　次

1 Introduction

Runaway electrons are formed under following two plasma conditions in tokamak plasma devices; (1) During low density discharges, some of the electrons in the plasma are accelerated further by the toroidal electric field without losing the energy by collisions with the other particles. Since the cross section decreases with increasing energy, the electron can "runaway" in energy. (2) During a disruption, the electrical field is so high that this runaway acceleration condition can develop even at normal plasma densities. As runaway electrons travel around the tokamak, they continue to be highly accelerated to energies of several MeV and more until they interact with PFCs (Plasma Facing Components) in a highly localized area. Because of their high energy, the electrons penetrate several centimeters into the material as they slow down and generate a very large volumetric heat in the components. Possible consequences are melting or material damage induced by steep temperature gradients. An important difference to most disruption induced heat loads on PFCs surface is the large penetration depth of runaway electrons, which has a possibility to give significant heat loading to cooling tubes covered with a thick armor. Therefore, it is important to evaluate the thermal response of PFCs in the runaway electrons events.

1.1 Previous works

The experimental and numerical study on the runaway electrons events is reviewed comprehensively in Ref. 1. This review also included the description of the generation processes of runaway electrons in the tokamak and the interaction of high energy electrons and photons with the materials. It is impossible to calculate the heat generation caused by the high energy electrons penetrating material analytically, since the high energy electron produces a lot of secondary particles (positrons, electrons and photons), whose history is determined by probabilistic (quantum-mechanical) laws. Such events can be simulated by the computer codes which follow the primary particle in small steps, computing for each step the energy loss, multiple scattering and generation of secondary particles, which can again generate new particles, etc. Some computer codes are developed and widely used in high energy physics for qualitative simulation of the

interaction of high energy particles with the material using Monte Carlo method.

Here the numerical simulation for runaway electrons relevant to the PFC design are summarized. The first numerical analysis for the impact of runaway electrons on the PFCs was carried out by McGrath[2] using a Monte Carlo code ITS (Integrated TIGER Series)[3]. For high energy runaway electrons over 100 MeV, Calen et al.[4] performed a one and two dimensional simulation using Monte Carlo code GEANT3 developed by CERN[5]. They performed the computational simulation of the impact of the electrons with an energy range from 10 to 600 MeV and an angle of incidence onto the material within the range from 0.5 deg to 25 deg for carbon, molybdenum, steel and tungsten[4][6]. Niemer et al.[7] compared the simulation results of the runaway electrons from the PTA code package[8] performed with the experimental results by Bolt et al[9][10]. The PTA code package also includes the Monte Carlo code ITS[3]. Kunugi et al.[11] compared the results from EGS4 (Electrons Gamma Shower, Ver. 4) [12] with that from GEANT3, and showed preliminary for the three cases of proposed ITER/CDA (International Thermonuclear Experimental Reactor / Conceptual Design Activities) divertor models. The importance of including the magnetic field in the analysis was stressed by Bartels[13][14] and Kunugi[15]. It causes bending back of reflected charged particles caused by gyration of the electrons around the magnetic field lines. Generally, these codes can be used to describe the heat distribution in various PFC designs to predict the maximum surface heat load from runaway electrons. The accuracy of these codes is better than 20 %

1.2 Objectives and approach

All of the analyses mentioned in 1.1 estimated only the energy deposition or volumetric heat generated by impact of runaway electrons, which cause the temperature rise in the material[6][16]. From the simulation result for a simple First Wall model, i.e., 10 mm thick Be armor, 5 mm thick Cu and 10 mm thick SS layers, the temperature rise was predicted to reach over 900 K at the surface of Cu structure in case of the electron surface energy load of 40 MJ/m^2[16]. Such a thermal excursion will bring the serious damage to PFCs.

However, this temperature rise calculated in the adiabatic condition might be over-

estimated because the area irradiated by runaway electrons moves and the energy load onto the PFC surface decrease as a function of time. This behavior of runaway electrons is conjectured from the analogy of the spatial displacement and the energy decay of the tokamak plasma during a plasma disruption. Recently, re-estimation of the energy load distribution of runaway electrons onto the PFC surface was made by S. Putvinski[17]. His estimation will be summarized in Sec. 2. An usual Monte Carlo simulation mentioned above could not treat the transient behavior of runaway electrons.

The other disadvantage of the previous simulations was that they could not include the cooling effect despite that the ITER PFCs have the cooling system. It is possible to improve these issues by developing the integrated numerical code consisted of the Monte Carlo method for the coupled electrons and photon transport analysis and the finite element method for the thermo-mechanical analysis of PFCs. The integrated code like this can deal with the transient response of PFCs irradiated by runaway electrons, if the time-dependent condition of the electron flux is provided as mentioned above.

The objectives of this study are (1) to develop an integrated code system of the Monte Carlo method and the finite element method for the more practical simulation for runaway electron event, (2) to make a time-dependent flux condition of runaway electron based on Putvinski's estimation, and (3) to assess the loss of the ITER PFCs in runaway electron event using the results of (1) and (2).

In the present paper, we first summarize Putvinski's estimation for the energy load and the time-dependent flux condition of runaway electrons on PFCs. After a brief description of our code system, the thermal response of PFCs caused by runaway electron are examined. Then we estimate the loss or melting depth of PFCs caused by the impact of runaway electron.

2 Estimation of Heat Load on Plasma Facing Components Produced by Runaway Electrons during Plasma Disruption for ITER

The thermal response of plasma facing materials during interaction with MeV-electrons is determined by the electron energy, the density of the material, the electron flux and

the flux distribution. However, there had been no reasonable estimation for the electron flux and its distribution so far. Recently, S. Putvinski made the estimation of heat load on PFCs produced by the runaway electrons during plasma disruption base on the updating plasma modeling[17]. Here, his estimation of heat load should be summarized and then we introduce the electron flux and its distribution according to his estimation.

2.1 Summary of Putvinski's estimation for heat load by Runaway Electrons

If the runaway electrons will be well confined during the current quench phase of a plasma disruption in ITER then one can expect a generation of large runaway current up to 15 MA. Total kinetic energy of runaway electrons (average particle energy 12.5 MeV) carrying 15 MA is only 30 MJ. The previous specifications were based on this figure and on an assumption that runaway electrons will be deposited on toroidally symmetric area with poloidal width of 0.2 m – 0.5 m defined by plasma vertical motion. The peak heat load was estimated as 5 MJ/m^2.

However, recent modeling has shown that a large fraction of magnetic energy of the runaway current can be transformed to additional runaway electrons during VDE (Vertical Displacement Event). As the result the upper limit for total runaway electron energy was elevated from previous 50 MJ to a new range 30 – 300 MJ. In the following memo the peak heat load was re-estimated including effect of toroidal misalignment of the wall.

We shall introduce runaway electron impact (grazing) angle with the wall surface, $\alpha = p_\perp/p$, where $p_\perp$ is component of electron momentum perpendicular to the wall, and shall estimate the peak heat load as function of this parameter. The SOL thickness can be evaluated as

$$\Delta = 2\pi R\alpha$$

and poloidal length of instantaneous distribution as

$$x_{pol} = \sqrt{2\pi Ra\alpha}. \tag{1}$$

For the sake of simplicity we assume that distribution of normal to the wall heat

Table 1: Tentative Specifications for Runaway Electrons

Parameter	Range	Reference value
Average energy of electrons, E_0 [MeV] $f(E) \sim \exp(E/E_0)$	10 – 15	12.5
Total kinetic energy deposited on the wall, W_{RE} [MJ]	30 – 300	150
VDE time, τ_{VDE} [sec]	0.05 – 1	0.15
Displacement of plasma wall contact point, x_s[m]	0 – 1	0.5
Amplitude of plasma wall misalignment, Δ [m]	0 – 0.1	0.05
Impact angle, α [degrees]	10^{-5} – 1	0.01

flux has Gaussian shape:

$$q(x,t) = \frac{W_{RE}}{\pi\, x_{tol}\, x_{pol}\, \tau_{VDE}} \exp\left(-\frac{(x - x_{cen}(t))^2}{x_{pol}^2} - \frac{t^2}{\tau_{VDE}^2}\right) dxdt. \qquad (2)$$

Here x_{tor} is effective toroidal length of the distribution, τ_{VDE} is the time duration of the heat load, $x_{cen}(t)$ is poloidal coordinate of plasma wall contact point which is moving along the wall during VDE. The distribution is normalized on the total energy of runaway electrons.

The peak heat load described by the above formula increases in time with characteristic time τ_{VDE}, reaches maximum at $t = 0$ and then decays. If one chose poloidal coordinate x such as $x_{con}(0) = 0$ then Eq. (2) can be rewritten as follows:

$$q(x,t) = \frac{W_{RE}}{\pi\, x_{tor}\, x_{pol}\, \tau_{VDE}} \exp\left(-\frac{(x - x_s t/\tau_{VDE})^2}{x_{pol}^2} - \frac{t^2}{\tau_{VDE}^2}\right) dxdt. \qquad (3)$$

Here x_s is magnitude of plasma displacement along the wall. Toroidal width of the distribution is defined by misalignment of the plasma surface and the First Wall. Here we shall consider only effect of large scale, $n = 1$, perturbations. In this case effective toroidal length of the distribution, x_{tor}, can be easily estimated $x_{tor} = \sqrt{2\pi R^3 \alpha/\Delta}$, where Δ is amplitude of plasma displacement. The cause of $n = 1$ displacement can be either misalignment of the wall or distortion of the plasma shape by MHD perturbations. In the following estimation we shall use a slightly modified expression

for toroidal width:

$$x_{tor} = \frac{2\pi R(\sqrt{2\pi R^3\alpha/\Delta} + d)}{2\pi R + \sqrt{2\pi R^3\alpha/\Delta}}, \tag{4}$$

which takes into account that x_{tor} has the upper limit $2\pi R \approx 50$ m, and the lower limit, d, equal to toroidal length of one blanket module, $d \approx 1$ m.

Eq. (3) gives estimate for maximum power load

$$q_{max} = \frac{W_{RE}}{\pi\, x_{tol}\, x_{pol}\, \tau_{VDE}}, \tag{5}$$

and energy load:

$$p_{max} = \int q(0,t)\, dt = \frac{W_{RE}}{\sqrt{\pi}\, x_{tor}\, (x_s^2 + x_{pol}^2)^{1/2}}. \tag{6}$$

For estimations of the peak heat loads we shall adopt the specifications for runaway electrons tabulated in Table 1. The peak energy load given by Eq. (1), (4) and (6) as function of the impact angle, α, calculated for the reference parameters from Table 1.

2.2 Estimation for Runaway Electron flux and its distribution

When one perform the simulation for runaway electron impact on PFCs, it is necessary to estimate the electrons flux and its distribution. If the PFC treated in the simulation is exposed to the maximum heat flux at $t = 0$, i.e., at the start of VDE or disruption, that is, the poloidal coordinate is chosen as $x = 0$. In this case, the electron flux and its distribution can be given from Putvinski's estimation as follows:

The heat flux distribution at $x = 0$ is rewritten from Eq. (3) as :

$$q(0,t) = \frac{W_{RE}}{\pi\, x_{tor}\, x_{pol}\, \tau_{VDE}} \exp\left(-\frac{x_s^2 + x_{pol}^2}{x_{pol}^2\, \tau_{VDE}^2}\, t^2\right). \tag{7}$$

We will describe the particle flux of runaway electron as function of time after this formulation. If the energy spectrum of runaway electron is also considered, the particle flux with the kinetic energy E at the time t, $n_{RE}(t, E)$, can be expressed as follows:

$$n_{RE}(t,E) = D \exp\left(-\frac{x_s^2 + x_{pol}^2}{x_{pol}^2\, \tau_{VDE}^2}\, t^2\right) \exp\left(-\frac{E}{E_o}\right), \tag{8}$$

where D is a proportional constant. We can estimate the total energy flux of the incident electrons by integrating Eq. (8) over the time and the energy spectrum;

$$\text{RE energy flux } [\text{J/m}^2] \;=\; \int_0^\infty \int_{E_o}^\infty E n_{RE}(t,E)\, dE\, dt$$

$$= D\int_{E_o}^{\infty} E\exp\left(-\frac{E}{E_o}\right)dE\int_0^{\infty}\exp\left(-\frac{x_s^2+x_{pol}^2}{x_{pol}^2\,\tau_{VDE}^2}\,t^2\right)dt$$

$$= DE_o^2\exp(-1)\sqrt{\pi}\frac{x_{pol}\,\tau_{VDE}}{(x_s^2+x_{pol}^2)^{1/2}}. \tag{9}$$

This value must be equal to the energy load,P_{max}(Eq.(6)), estimated by Putvinski. The total flux of runaway electrons at the time t can be calculated as follows :

$$n_{RE}(t)\ [1/\mathrm{m^2s}] = \int_{E_o}^{\infty} D\exp\left(-\frac{E}{E_o}\right)\exp\left(-\frac{x_s^2+x_{pol}^2}{x_{pol}^2\,\tau_{VDE}^2}t^2\right)dE$$

$$= DE_o\exp(-1)\exp\left(-\frac{x_s^2+x_{pol}^2}{x_{pol}^2\,\tau_{VDE}^2}t^2\right). \tag{10}$$

Eliminating D from Eq.(10) using Eqs.(5), (6) and (9), the number flux of runaway electrons with the energy of E at time t can be describe as :

$$n_{RE}(t,E) = \frac{P_{max}\,(x_s^2+x_{pol}^2)^{1/2}}{E_o\,\sqrt{\pi}\,x_{pol}\,\tau_{VDE}}\exp\left(-\frac{x_s^2+x_{pol}^2}{x_{pol}^2\,\tau_{VDE}^2}t^2\right)\mathrm{Pn}(E), \tag{11}$$

$$= \frac{W_{RE}}{E_o\,\pi\,x_{tor}\,x_{pol}\,\tau_{VDE}}\exp\left(-\frac{x_s^2+x_{pol}^2}{x_{pol}^2\,\tau_{VDE}^2}t^2\right)\mathrm{Pn}(E), \tag{12}$$

$$= \frac{q_{max}}{E_o}\exp\left(-\frac{x_s^2+x_{pol}^2}{x_{pol}^2\,\tau_{VDE}^2}t^2\right)\mathrm{Pn}(E), \tag{13}$$

here, $\mathrm{Pn}(E)$ is a probability distribution function of runaway electrons with the energy of E as defined by the following

$$\mathrm{Pn}(E) = \frac{\exp(-E/E_o)}{\int_{E_o}^{\infty}\exp(-E/E_o)\,dE} = \frac{\exp(-E/E_o)}{E_o\,\exp(-1)} \tag{14}$$

.If one specifies one of W_{RE}, P_{max} and q_{max} as well as the other parameter concerning length and time, the number flux of runaway electrons can be determined.

These estimation is appropriate in case that the poloidal coordinate is chosen as $x = 0$. It is easy to improve the estimation in the arbitrary poloidal coordinate of PFCs.

3 Analysis Procedures

Here the integrated numerical code are introduced, which is consisted of the Monte Carlo method for the coupled electrons and photon transport analysis and the finite

element method for the thermo-mechanical analysis of PFCs. This integrated code can deal with the transient response of PFCs irradiated by runaway electrons by using the time-dependent condition of the electron flux is provided as mentioned in Sec. 2.1.

3.1 Description of codes

The set of codes, PATREN, EGS4 and ABAQUS are used to simulate runaway electrons impact on PFCs.

PATREN is used to generate the model geometry and finite element mesh. ABAQUS is a general purpose finite element code capable of performing a wide range of non-linear applications such as heat transfer and stress analysis.

EGS (Electron Gamma Shower) code system is a general purpose package for the three dimensional Monte Carlo simulation of the coupled transport of electrons and Photons[12]. The most recent enhanced version is called EGS4. EGS4 system can simulate the electromagnetic processes, and the transport of electrons and photons in arbitrary geometry for the case of a particle energy above a few KeV up to several TeV.

The electromagnetic physics models used in EGS4, especially the multiple scattering model formulated by Bethe[18], is based on the Moliére's theory which neglects a lateral change of the position in the step of the electron transport. The available step lengths are calculated automatically, while still multiple scattering is taken into account.

For the purpose to generate material data such as the energy-dependent cross section of electrons and photons for EGS, a stand alone utility program, PEGS code (Preprocessor for EGS) is used. This code can calculate the material data at the specified density of the material.

Some modifications were done by K. Kunugi[15] in order to the re-entry behavior of runaway electrons after reflections from the PFCs caused by the magnetic field effect in the vacuum near the materials. In this version, the magnetic field is assumed to be uniform and one-dimensional.

Some functions are added for this simulation in EGS4. One is a function which take the incident energy distribution of the runaway electrons into account. This dependency can obey the arbitrary form, especially, the exponential form, $\exp(-E/E_o)$

as in Tab. 1.

The other is the interface between Monte Carlo code, EGS4 and finite element code, ABAQUS. The output data from EGS4 is the statistical averaged amount of the energy deposition in each element of ABAQUS.

How our code system works for an analysis about PFC model is as follows : The necessary material data for EGS4 is calculated for the PFC material with PEGS. A two dimensional geometry and finite element mesh of the PFC model is generated with PATRAN. This finite elements mesh is used as the geometry input for EGS4. EGS4 calculates the energy deposition in the three dimensional model. This energy deposition is reduce to the two dimensional finite element and then used as a volumetric heat source in ABAQUS. ABAQUS calculates the transient temperature distributions in the model.

3.2 Assumptions

The following assumptions are used in this study;

1. Temperature dependency of the density and cross section of material are neglected.

2. The energy deposition in the coolant of the PFC model is not considered in ABAQUS, because the heat transfer coefficient is defined at the inside surface of the cooling tube.

3. The energy spectrum of the incident electrons keeps same shape during a disruption. One of the results from EGS4 is the statistical averaged value of the energy deposition caused by one electron incidence. Then the incident particle flux of runaway Electrons into the surface of the armor tile can vary as a function of time, which must be specified in the input data of ABAQUS.

4. We treat the PFC model which is exposed to the maximum heat flux at the start of VDE or disruption, $t = 0$, that is, the poloidal coordinate is chosen as $x = 0$. In addition, the heat flux or particle flux of runaway electrons onto the surface of the PFC model is uniform.

4 Results and Discussions

4.1 Simulation model for divertor and first wall of ITER / EDA

The runaway electrons impact simulation were performed for three types of the model for proposed ITER/EDA (Engineering Design Activities) plasma facing components, (a) first wall(FW) with beryllium (Be) armor and divertors with (b) CFC (Carbon-Fiber-Composite) and (c)tungsten (W) armor as shown in Figure 1 with two dimensional simplification. The magnetic filed was parallel to the top surface of the model and its magnitude was equal to 6 T according to ITER condition. The electrons collided with the surface with a incident angle of 0.01 deg. The periodic boundary conditions were applied in x and y directions and the vacuum region was assumed in both z direction in the EGS4 calculations. In the ABAQUS calculations, the adiabatic boundary conditions were used in all direction except for the top surface of the model. The top surface was assumed to be received the constant heat flux as the steady state operation, such as 0.5 MW/m^2 for the first wall and 5 MW/m^2 for divertor. At cooling tube wall, the heat transfer coefficients of the smooth tube for the first wall and of the swirl tube for the divertor were given and the ambient temperature of cooling water is 140 °C.

The conditions for runaway electrons impact were assumed as those of the reference value listed in Table 1. The energy load of runaway electrons were ranged from 10 to 75 MJ/m^2 for each model.

4.2 Heat generation inside of ITER Plasma Facing Components caused by runaway electron impact

The effects of the magnetic field and the incident angle between runaway electron and the surface on the heat generation in the simplified model were already discussed elsewhere[14][15]. Here we introduce only the profiles of the volumetric heat generated by runaway electron impact in the three types of ITER/EDA PFCs, FW with Be armor and divertor with CFC and W armors in Fig 2. We also discuss about the dependency of the heat generation on spatial mesh of the EGS4 to use statistically averaging physical values in Appendix.

The incident energy density of runaway electrons was 50 MJ/m^2 and the incident

angle between the runaway electrons and PFC's surface was 0.01 deg. These profiles indicate those at the start of the runaway electrons event, i.e., $t = 0$. Those volumetric heat generation decrease according to Eq. (7) and become almost zero at 10 ms after the start of the runaway electrons events.

The maximum value of heat generation near W armor surface was largest among three PFC models because of its large stopping power to high energy electrons. CFC and Be armors had almost same profile of the heat generation since their densities were almost same.

4.3 Thermal response of Plasma Facing Components

Figures (3), (4) and (5) show the temperature profiles at the edge of the surface of each PFC models in various incident runaway electrons energy densities. From these figures, the temperatures at the surface in each condition reached the maximum value after about 50 ms after the start of the runaway electrons impact since the electron flux decreased rapidly with time as discussed in Sec. 2.

Although the phase change of the material was not taken into account in this analyses, we might estimate the melting region of the armor of PFCs roughly. For this purpose ,we defined that the melting depth of material was the region whose temperature exceeded the melting point. In order to determine the melting depth when the surface temperature reaches the maximum value, the isotherm contours and the temperature profiles along the edge line of the PFCs model at 50 ms after the start of the runaway electrons impact with the incident angle of 0.01 deg are shown in figures 6 – 11. From these results, a high temperature region exist very near the armor surface in each PFC model at 50 ms after the start of the runaway electrons impact.

In case of the CFC-armor divertor model, the maximum temperature was less than the sublimation point of graphite even if the energy density of the runaway electrons was 75 MJ/m^2. It is considered that the surface of the armor dose not suffer from the serious damage such as sublimation.

On the other hand, the surface temperatures of the FW and W-armor divertor model exceed the melting point of the armor material with the energy density of 50 MJ/m^2 and and 20 MJ/m^2, respectively. The melting depth of each model was

estimated to be about 0.5 mm for Be armor and 0.3 mm W armor.

It has been considered so far that one of the possible consequences of runaway electrons event is melting of heat sink or burn-out at the cooling tubes. Our numerical simulations showed, however, that the temperatures at the Cu heat sink and cooling tube were less than the melting point in each PFC models shown in Figs. 6, 8 and 10, although the surface of the armor was melted.

5 Summary

The runaway electron effects on three types of ITER/EDA PFCs, the First Wall (FW) with Be armor and the divertors with CFC and W armors are studied parametrically by the numerical analyses. For the investigation of time-dependent thermal response of PFCs caused by runaway electrons impact, we developed an integrated numerical code, which consists of the Monte Carlo code, EGS4, for the coupled electrons and photons transport analysis and the finite element code, ABAQUS, for the thermo-mechanical analysis. In this code, we apply the realistic incident parameters and distribution of runaway electrons proposed by S. Putvinski, which can express the time-dependent behavior of runaway electrons, that is, movement of the area irradiated by runaway electrons and decay of the energy load onto PFCs surface as a function of time. These behavior of runaway electrons comes from the analogy of the spatial displacement and the energy decay of plasma during a plasma disruption.

In the present study, runaway electrons are assumed to impact onto PFC surface with the energy density ranging from 10 to 75 MJ/m^2, the average electron energy of 12.5 MeV, the incident angle of 0.01 deg and the characteristic time for decay of runaway electrons event of 0.15sec. From the numerical results, the maximum temperature of CFC armor is less than the sublimation point. Therefore, CFC armored divertor is considered not to suffer serious damage such as sublimation from runaway electrons impact with these conditions. On the contrary, the maximum temperatures of surfaces of FW and W-armored divertor models exceeded the melting point in case of the energy load of 50 MJ/m^2 and 20 MJ/m^2, respectively. In this simulation, we define the melting depth as the region where temperature is exceeded the melting point since the phase changes are not included in ABAQUS. By using this definition, the melting

depth is estimated to be about 0.5 mm for Be armor and 0.3 mm for W armor.

The most important result from our study is that heat sink and cooling pipe of each PFCs can be prevented from the melting or burn-out caused by runaway electrons impact, which is considered one of the possible consequences of runaway electrons event so far.

Acknowledgments

The authors would like to express their gratitude to Dr. Y. Okumura and other members of NBI heating Lab., Dr. H. Takatsu of Blanket Engineering Lab. and Dr. S. Putvinski of ITER JCT for their valuable discussions and comments. They would acknowledge Dr. M. Ohta and Dr. H. Kishimoto for their support and encouragement.

References

(1) H.-W. Bartels, T kunugi and A. J. Russo, "Runaway electrons effects," *J. Nucl. Fusion, Atomic-Plasma Interaction*, **5** (1994)225.

(2) R. T. McGrath, "Runaway electron analysis for TORE SUPRA," *Proc. of the Japan-U. S. Workshop P-92 on Plasma Material Interaction / High Heat Flux Data Needs for the Next Step Ignition and Steady State Devices*, Edited by A. Miyahara and K. L. Wilson, (1987) 435.

(3) J. B. Halbleib, et al., "ITS : The Integrated TIGER series of coupled electron / photon Monte Carlo transport codes," SAND84-0573.

(4) H. Calen, et al., "Energy deposition in tokamaks by impact of runaway electrons," Dept. of Radiation Science, Uppsla University, UU267, (1989).

(5) R. Brun, et al., "The GEANT3 electromagnetic shower program and a comparison with the EGS3 code," CERN report, DD/85-1, (1985).

(6) H. Bolt, et al., "Analysis of interaction of disruption induced components in next generation tokamaks," *J. Nucl. Sci. Technol.* **28**-9, (1991) 806.

(7) K. A. Niemer, et al., "Modeling of runaway electron damage for the design of tokamak plasma facing components," SAND 89-2405 (1990).

(8) K. A. Niemer, et al., "Computational and experimental modeling of runaway electron damage," SAND89-2304 (1990).

(9) H. Bolt, et al. "Runaway electron simulation by use of an electron linear accelerator," *J. Nucl. Mater.* **155-157** (1988) 256.

(10) H. Bolt, et al. "Simulation of tokamak runaway electron events," *J. Nucl. Mater.* **151** (1987) 48.

(11) T. Kunugi, et al., "The simulation of the energy deposition from runaway electrons in plasma facing components with EGS4," *Fusion Technol.* **21** (1992) 1868.

(12) W. R. Nelson, H. Hirayama, and D. W. O. Rogers, "The EGS4 code system," SLAC-265 (1985).

(13) H.-W. Bartels, "Interaction of relativistic electrons with Plasma Facing components," IPP-I/269, Max-Plank-Institut für plasmaphysik, (1992).

(14) H.-W. Bartels, "Impact of runaway electrons," *Fus. Eng. and Des.*, **23** (1993) 323.

(15) T. Kunugi, "Effects on runaway electrons on plasma facing components," *Fus. Eng. and Des.*, **23** (1993)329.

(16) L. N. Topilski, Private communication, (1997).

(17) S. Putvinski, Private communication, (1997).

(18) H. A. Bethe, "Molière's theory of multiple scattering," *Phys. Rev.* **89** (1953)1256.

Nomenclature

a	: plasma minor radius (= 2.8 m)
E	: kinetic energy of electrons [eV]
E_o	: average energy of electrons [eV]
n_{RE}	: incident number flux of runaway electrons [1/m^2/s]
p	: electron monentum
P_{max}	: maximum energy load caused by runaway electrons [J/m^2]
Pn	: probability distribution function
q	: heat flux [W/m^2]
R	: plasma major radius (= 8.14 m)
t	: time [sec]
x	: coordinate [m]
x_{con}	: poloidal coordinate of plasma wall contacting point [m]
x_{pol}	: poloidal length of distribution of runaway electrons [m]
x_s	: magnitude of plasma displacement along wall [m]
x_{tor}	: toroidal length of of distribution of runaway electrons [m]
W_{RE}	: total energy deposited on the wall caused by runaway electrons [J/m^2]

Greek symbols

α	: impact angle [degree]
Δ	: amplitude of plasma wall alignment [m]
τ_{VDE}	: VDE time [sec]

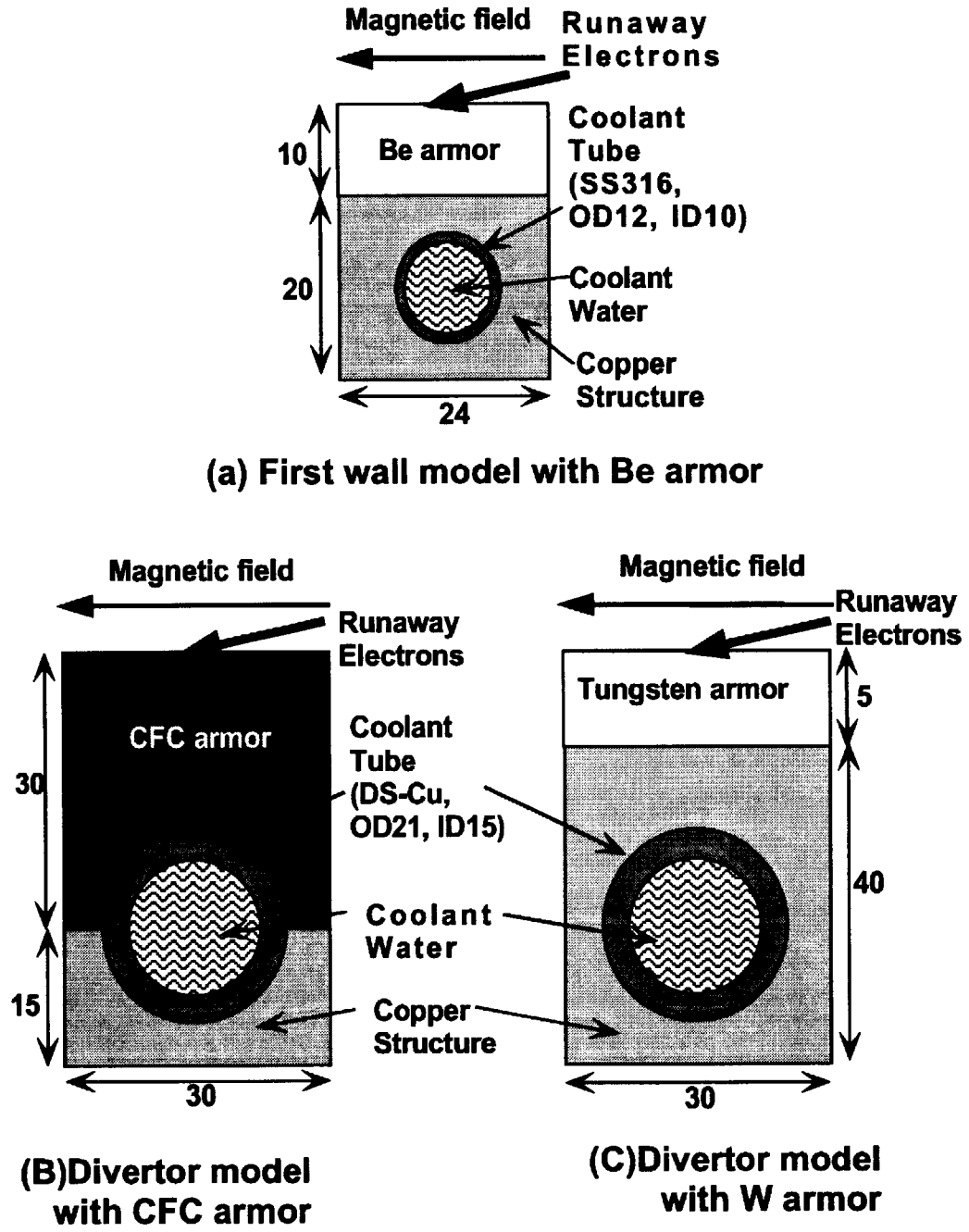

Figure 1: Three types of the simulation model for ITER/EDA PFCs, (a) First Wall and Divertors with (b) CFC armor and (c) Tungsten armor.

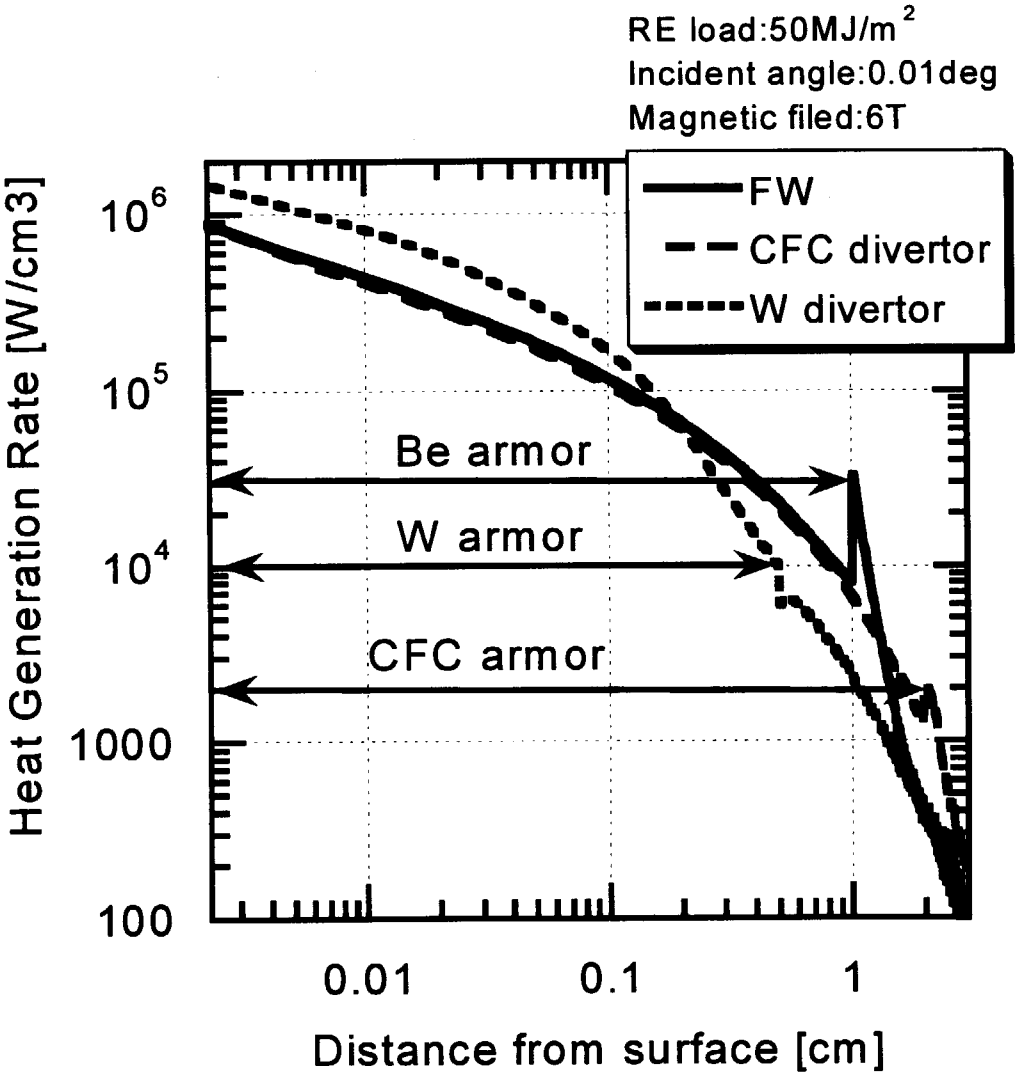

Figure 2: Profiles of heat generation in three types of PFCs, FW with Be armor and divertor with CFC and W armors due t runaway electrons impact with incident energy density of 50 MJ/m^2. Incident angle between runaway electrons and surface and magnetic field were 0.01 deg and 6 T.

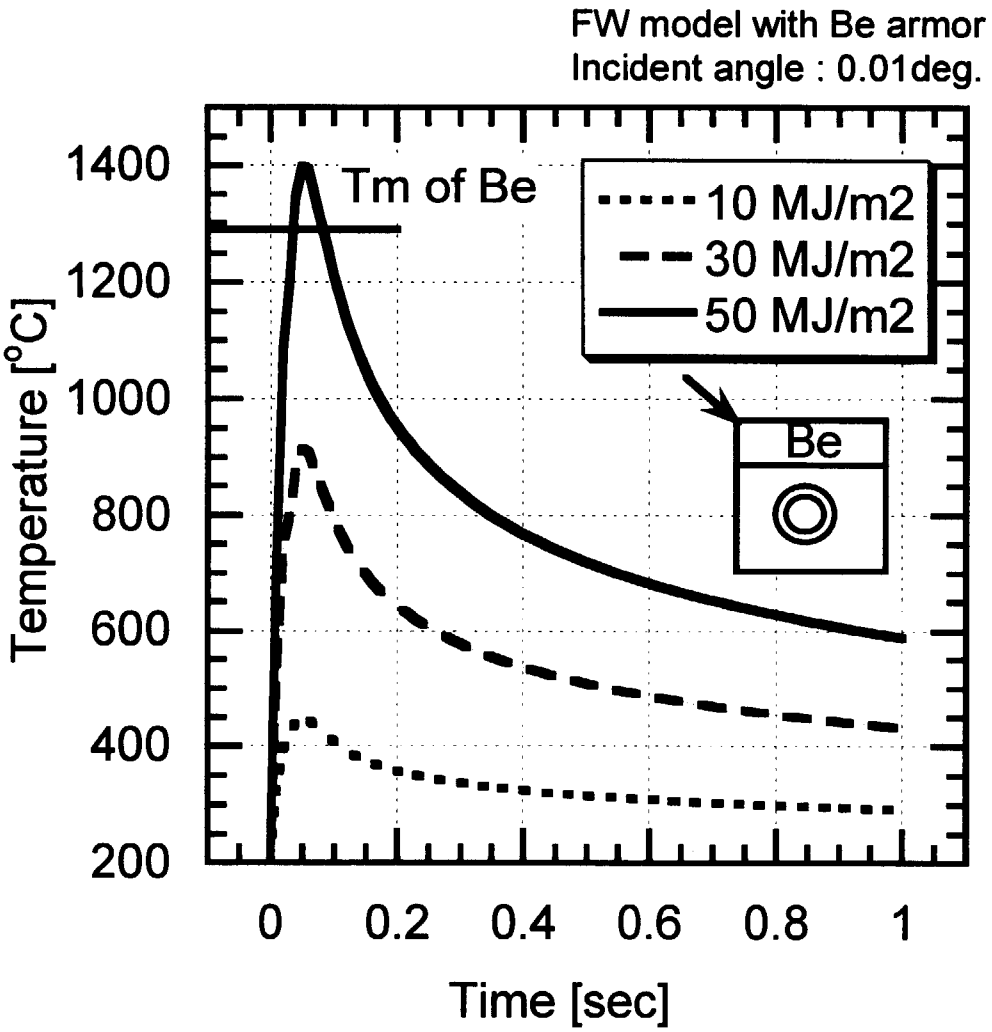

Figure 3: Temperature profiles at the edge of FW surface in three cases of incident energy density of the runaway electrons, 10, 30 and 50 MJ/m^2.

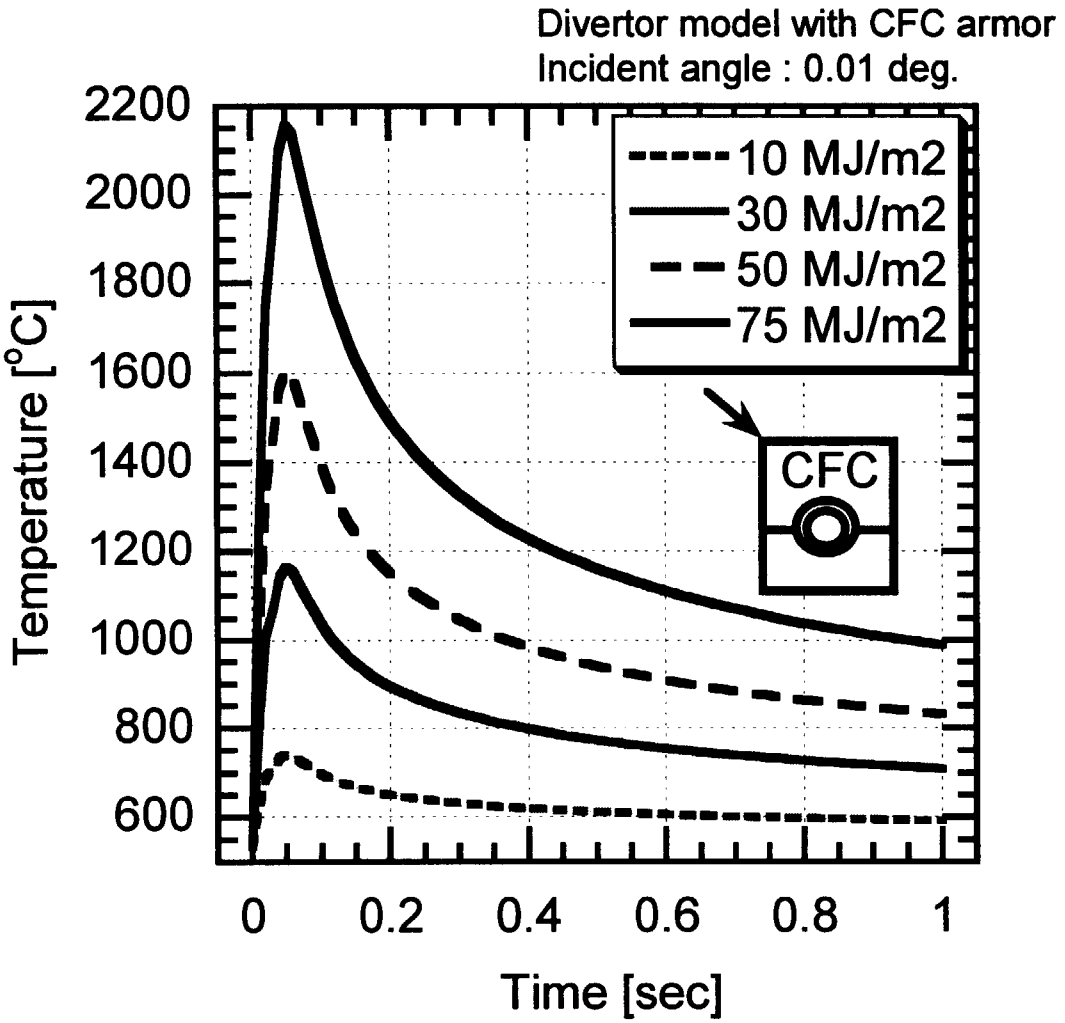

Figure 4: Temperature profiles at the edge of CFC surface in four cases of incident energy density of the runaway electrons, 10, 30, 50 and 75 MJ/m^2.

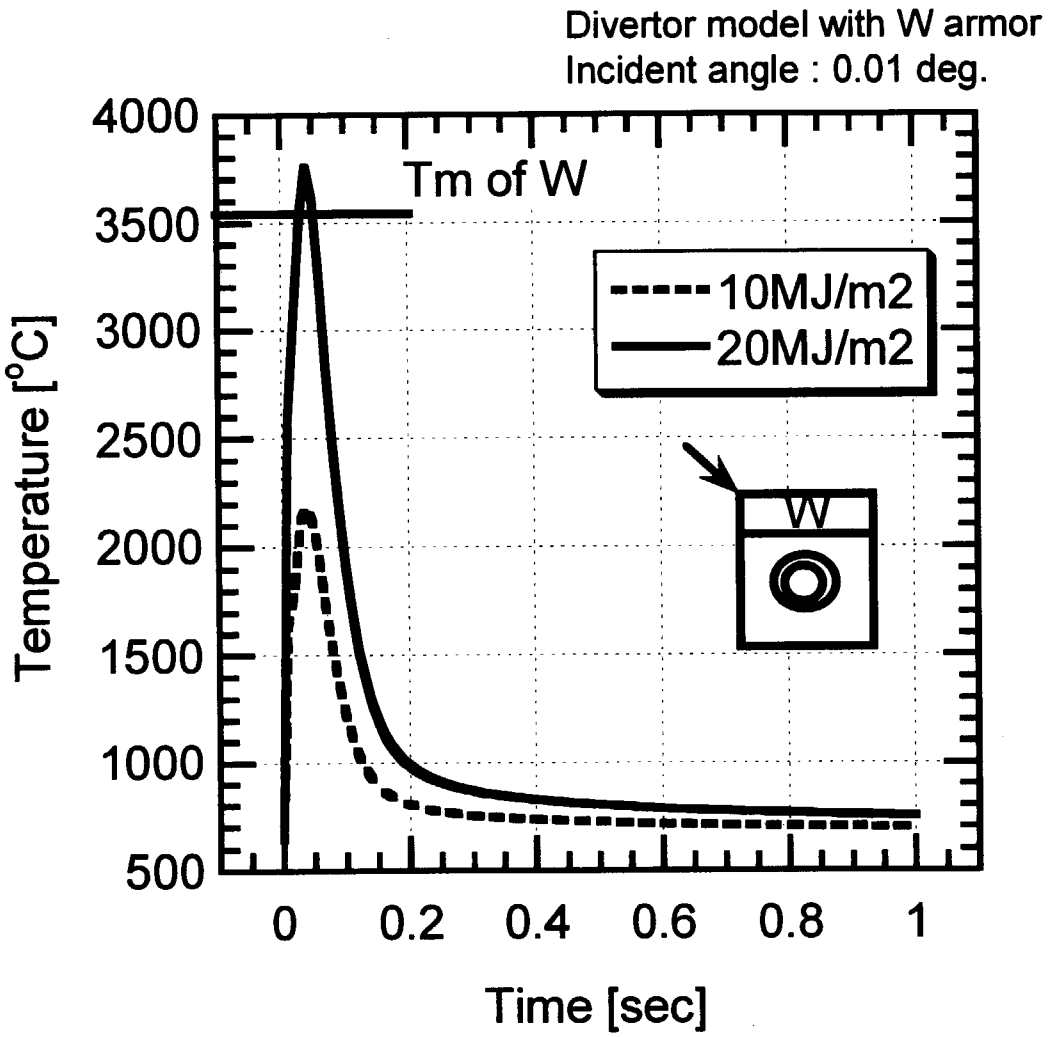

Figure 5: Temperature profiles at the edge of W surface in two cases of incident energy density of the runaway electrons, 10 and 20 MJ/m^2.

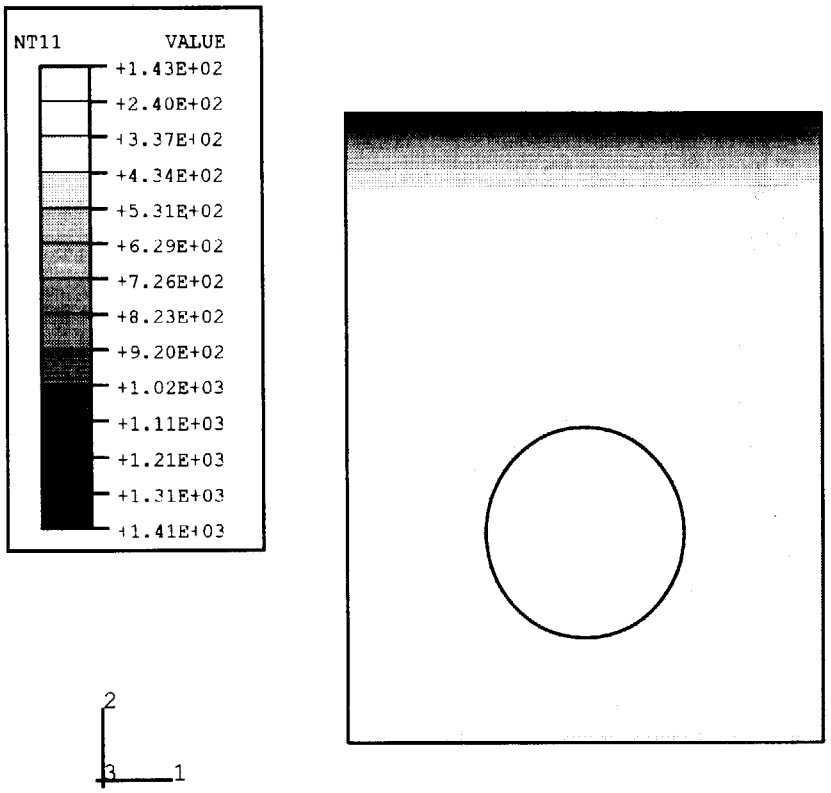

Figure 6: Temperature contour of FW with Be armor at 50 ms after start of runaway electron impact with the incident energy density of $50MJ/m^2$.

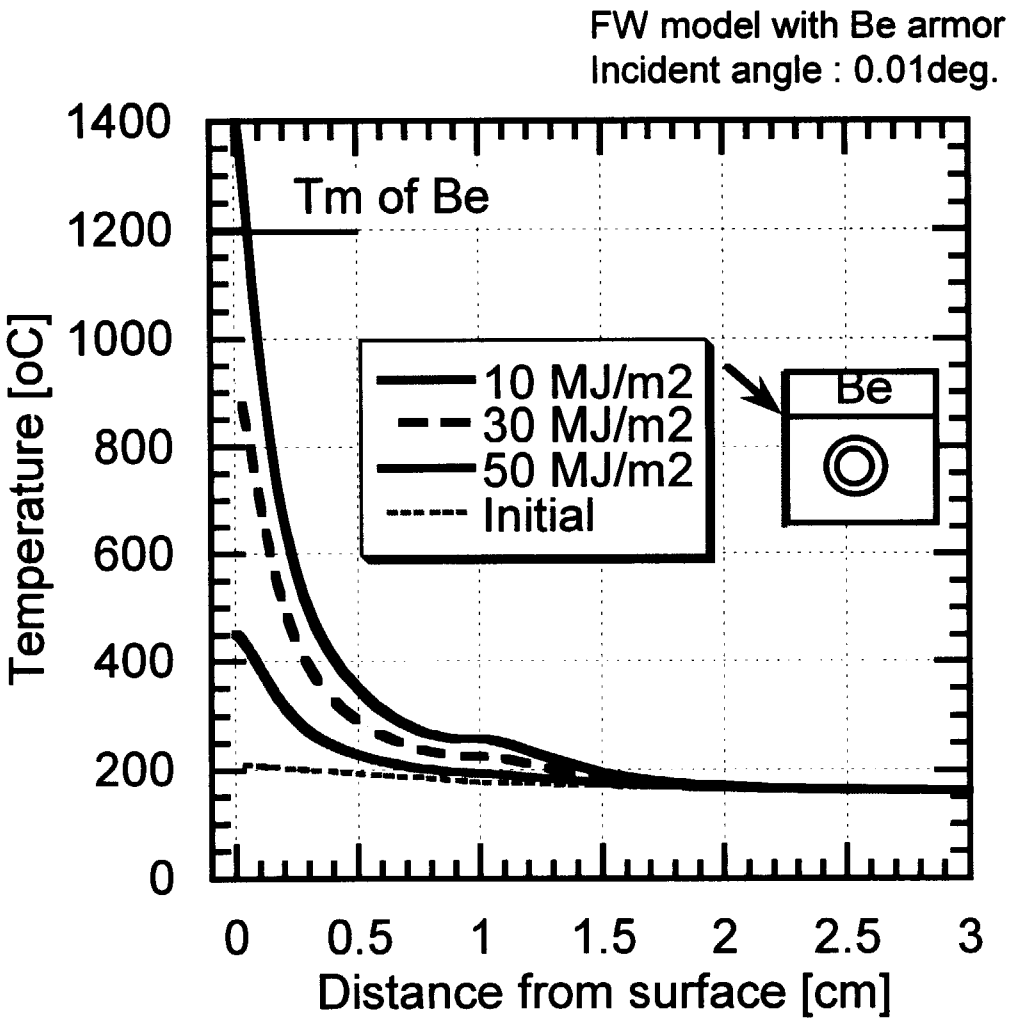

Figure 7: Temperature profiles on the edge line of FW with Be armor at 50 ms after the runaway electrons with the incident energy density of 10, 30 and 50 MJ/m^2.

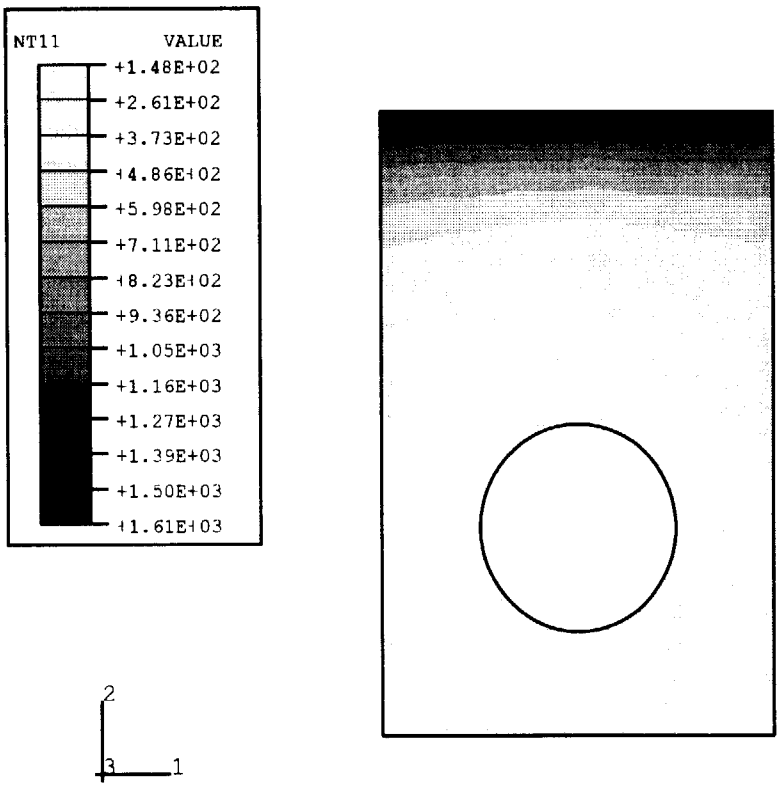

Figure 8: Temperature contour of divertor with CFC armor at 50 ms after the runaway electrons with the incident energy density of 50 MJ/m^2.

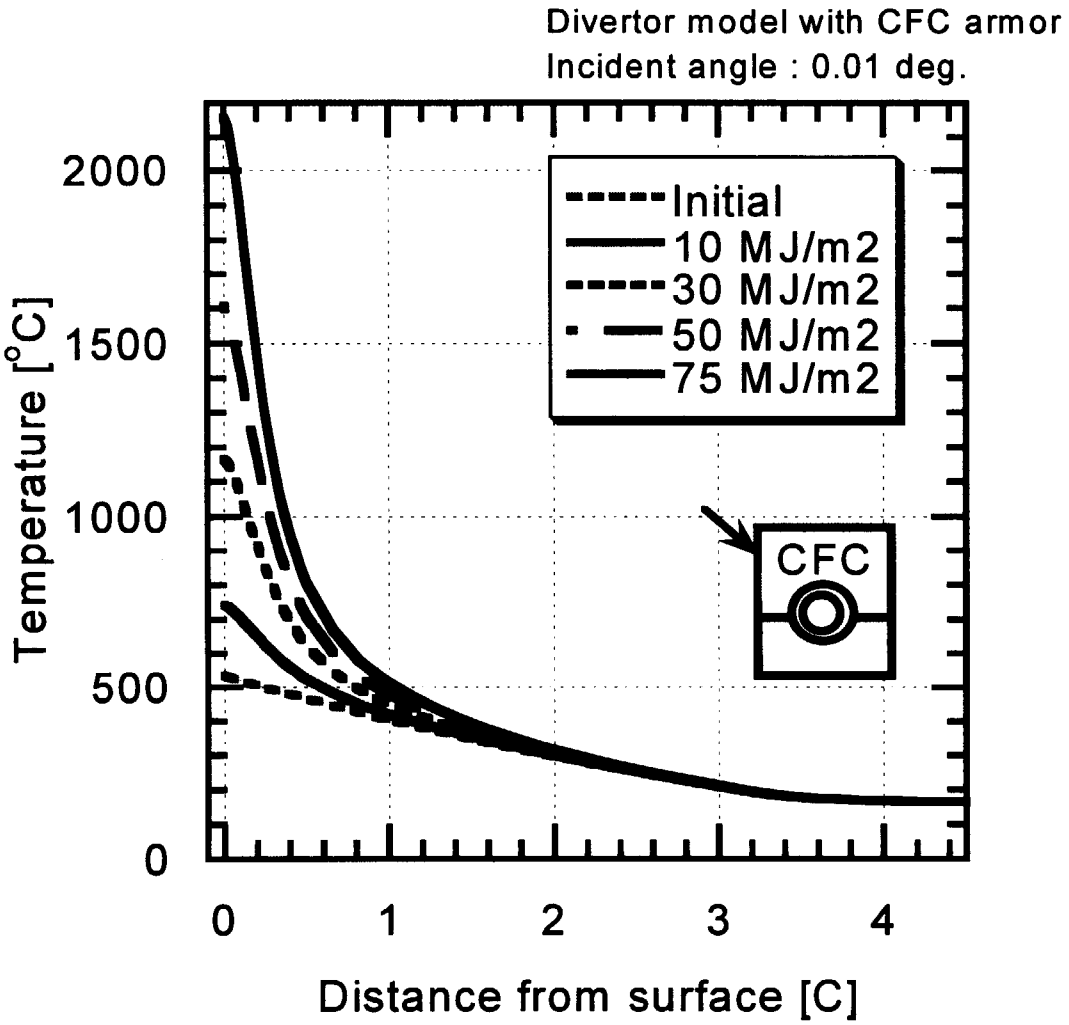

Figure 9: Temperature profiles on the edge line of divertor with CFC armor at 50 ms after the runaway electrons with the incident energy density of 10, 30, 50 and 75 MJ/m^2.

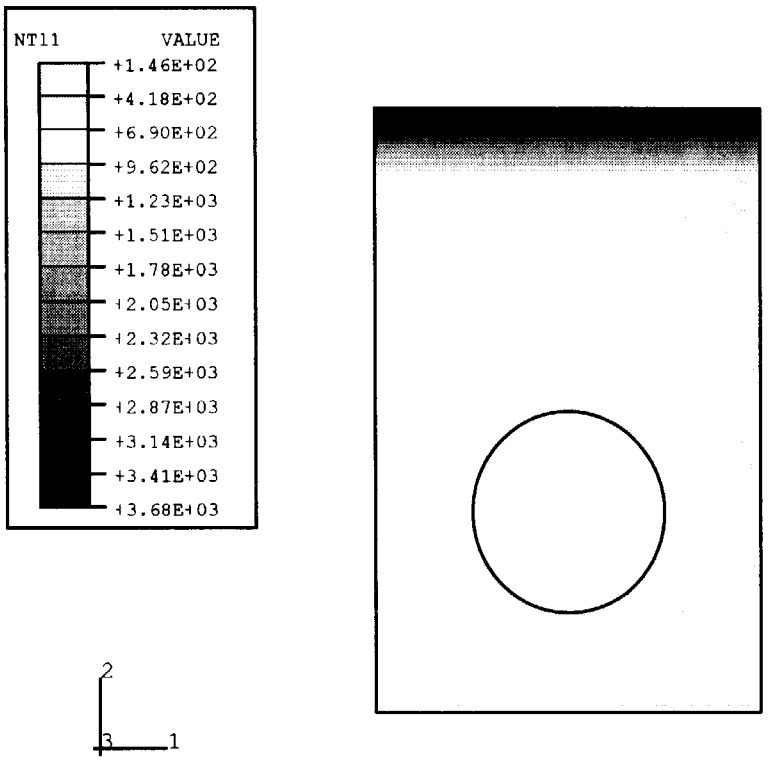

Figure 10: Temperature contour of divertor with W armor at 50 ms after the runaway electrons with the incident energy density of 20 MJ/m^2.

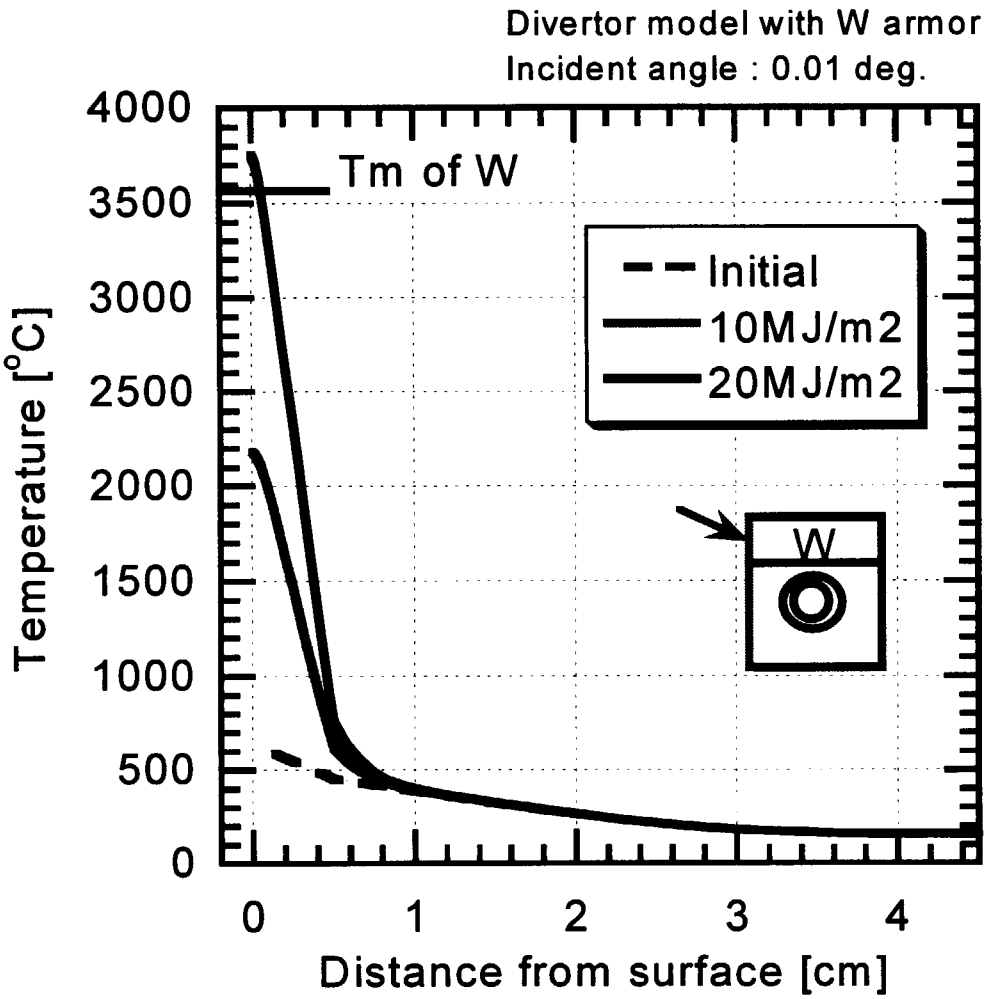

Figure 11: Temperature profiles on the edge line of divertor with W armor at 50 ms after the runaway electrons with the incident energy density of 10 and 20 MJ/m^2.

Appendix

A Dependency of EGS4 simulation on numerical mesh size and incident angle of electrons

In this appendix, we discuss about the dependency of the heat generation caused by runaway electrons on the numerical mesh size and incident angle of runaway electrons in EGS4 simulation.

It should be stressed that the EGS4 is Monte Carlo method, which dose not need the numerical mesh in order to trace the path of electrons and the photons in material and have no mesh dependency of the simulation itself. However, it is necessary to use the numerical mesh to calculate the statistically averaged physical values such as the heat generation caused by electrons as the results of the EGS4 simulation. This has possibility to bring the mesh dependency to thermal analysis with ABAQUS.

A.1 Dependency of heat generation and temperature profiles on numerical mesh size of EGS4

Figures A.1 and A.1 show the heat generation profiles in the FW model caused by runaway electrons with the incident energy of $50\mathrm{MJ/m^2}$ and incident angle of 0.01deg and 1deg, respectively, from the results of EGS4 simulation by using three types of mesh, $dx = 0.5\,\mathrm{mm}$, $0.12\,\mathrm{mm}$, and $0.03\,\mathrm{mm}$ (x is the normal direction to the armor surface). In both figures, the heat generations near the armor surface are estimated to be larger as the mesh size, dx, becomes fine. However, the profiles after the second mesh from the armor surface in case of $dx = 0.5\,\mathrm{mm}$ and $0.12\,\mathrm{mm}$ have almost same in case of $dx = 0.03\,\mathrm{mm}$. A possible reason of this characteristics of the profiles might be explained as follows: The variation of the heat generation caused by electrons is very steep in a thin region near the surface so that the resolution for the heat generation is not enough if the numerical mesh become thick.

In order to investigate the effect of differences of the heat generation near surface in the different mesh size on the thermal analysis, ABAQUS calculations are carried out in three difference sizes of the finite element, whose size near the surface are almost same as the above-mentioned EGS4 simulations, respectively as shown in Figs. A.3,

A.4 and A.5.

Figures A.3 and A.4 indicate the temperature profiles along the edge line of FW model at 50ms after the start of runaway electrons impact with the energy density of $50\,\mathrm{MJ/m^2}$ and incident angle of 0.01 deg (Figure A.4 emphasizes the armor surface region in Fig.A.3 using log scale as a horizontal axis). Figure A.5 shows a temperature history at the edge of the armor surface in the same condition of runaway electrons impact. The differences among them are very small and the profiles and history can be considered as same. From these results, we can confirm that there is no mesh dependency of EGS4 and ABAQUS simulations when the appropriate mesh size is used.

If the very thin mesh size is used for EGS4 simulation, it cost a huge calculation to get meaningful statistically averaged value with enough small deviation, for example, number of test particles for the electrons in case of the mesh size $dx = 0.03\,\mathrm{mm}$ is more than five million in this study. All results in Sec. 4 are derived from the simulation with the mesh size corresponding to $dx = 0.12\,\mathrm{mm}$.

A.2 Dependency of heat generation on incident angle between electrons and armor surface

In order to investigate the effect of the incident angle between the runaway electrons and the armor surface on the heat generation caused by electrons, EGS4 simulation with the numerical mesh size of $dx = 0.03$ mm were carried out for the various incident angle as shown in Fig. A.6. The magnetic field was assumed to be parallel to the armor surface.

The clear dependency of the heat generation on the incident angle appears when the incident angle is larger than 1 deg. As the incident angle is larger, the heat generation in the surface region become smaller. Compared with this tendency, there is little difference of the heat generation between the incident angle of 0.1 deg and 0.01deg. One of reasons is considered that this mesh size does not have enough resolution to grasp the steep variation of heat generation in the armor surface region as mentioned in Appendix A.1. Provided that the electron penetrates straight without any interaction into the armor with the incident angle of 0.01 deg, penetrating distance normal to

the surface is about 5 μm, while the electrons passes through the width of the FW model(= 2.4 cm). It might be necessary to use the mesh size of 5 μm in order to differentiate the dependency of the heat generation on the incident angle between 0.1 deg and 0.01 deg. The other reason considered as the re-entry motion of the electron, which is reflected at the armor surface. When the incident angle of electron is small, the possibility that the electron is reflected at the surface become large. The reflected electron can impact again with Larmor motion caused by the magnetic field parallel to the surface. However, the incident angle of re-entry electron after reflection can be conjectured to be random. Therefore, the dependency of the heat generation on the small incident angle of runaway electron is not remarkable.

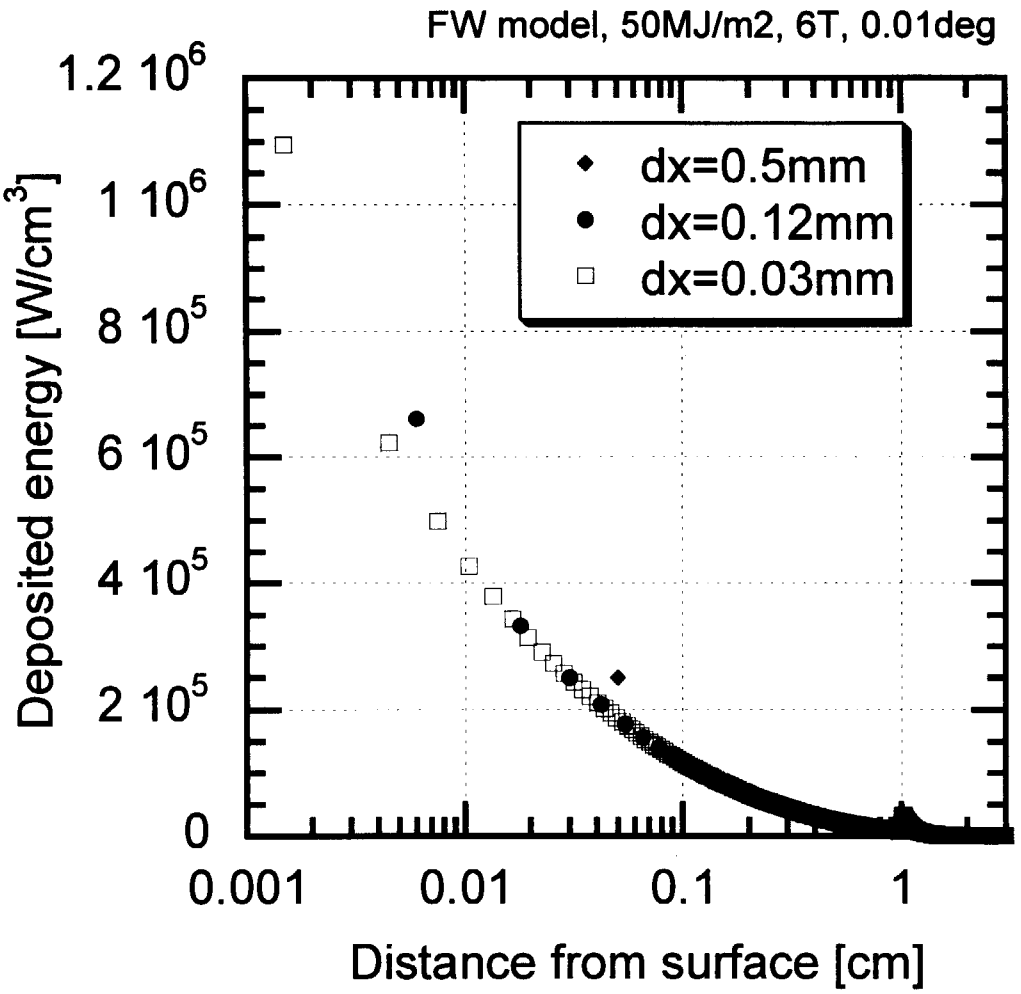

Figure A.1: Profiles of the heat generation in FW model from the results by using three mesh size of EGS4, $dx = 0.5\,\mathrm{mm}$, $0.12\,\mathrm{mm}$, and $0.03\,\mathrm{mm}$. Incident angle and magnetic field are $0.01\,\mathrm{deg}$ and $6\,\mathrm{T}$.

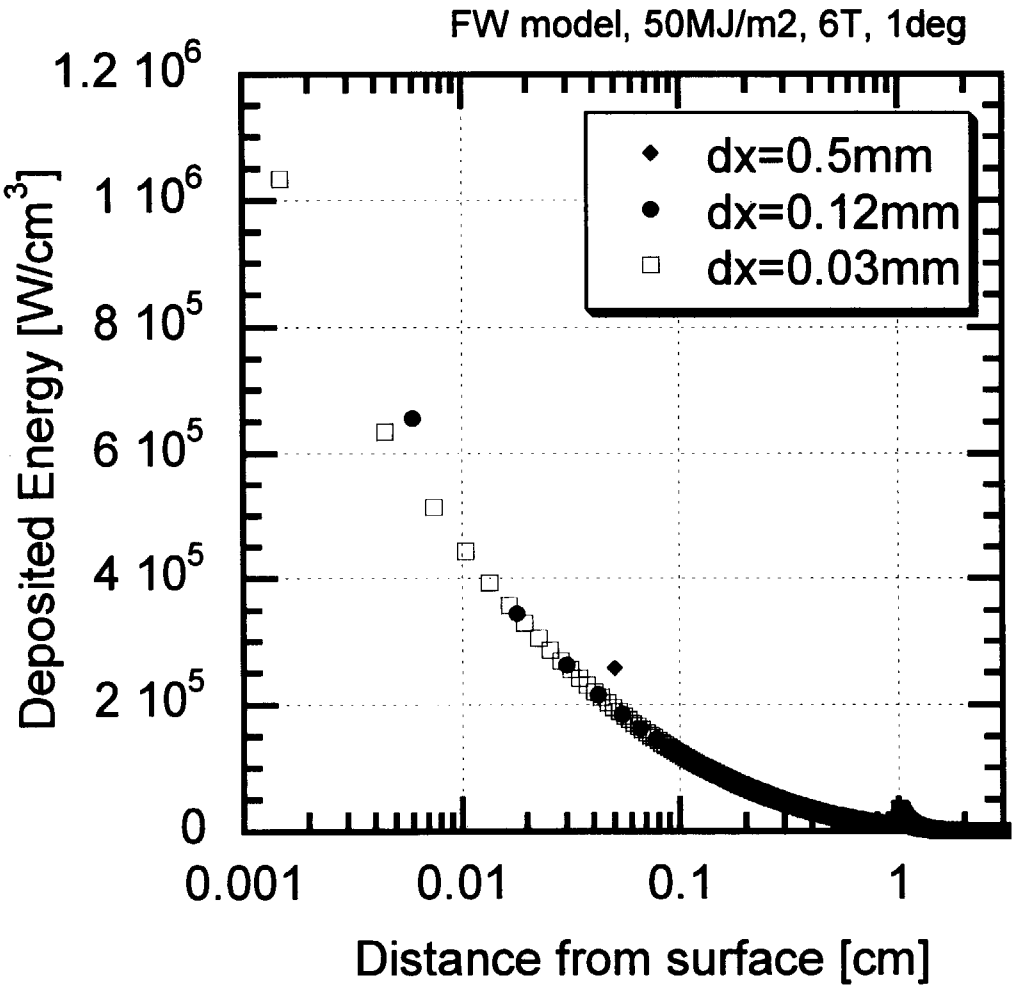

Figure A.2: Profiles of the heat generation in FW model from the results by using three mesh size of EGS4, $dx = 0.5\,\mathrm{mm}$, $0.12\,\mathrm{mm}$, and $0.03\,\mathrm{mm}$. Incident angle and magnetic field are 1 deg and 6 T.

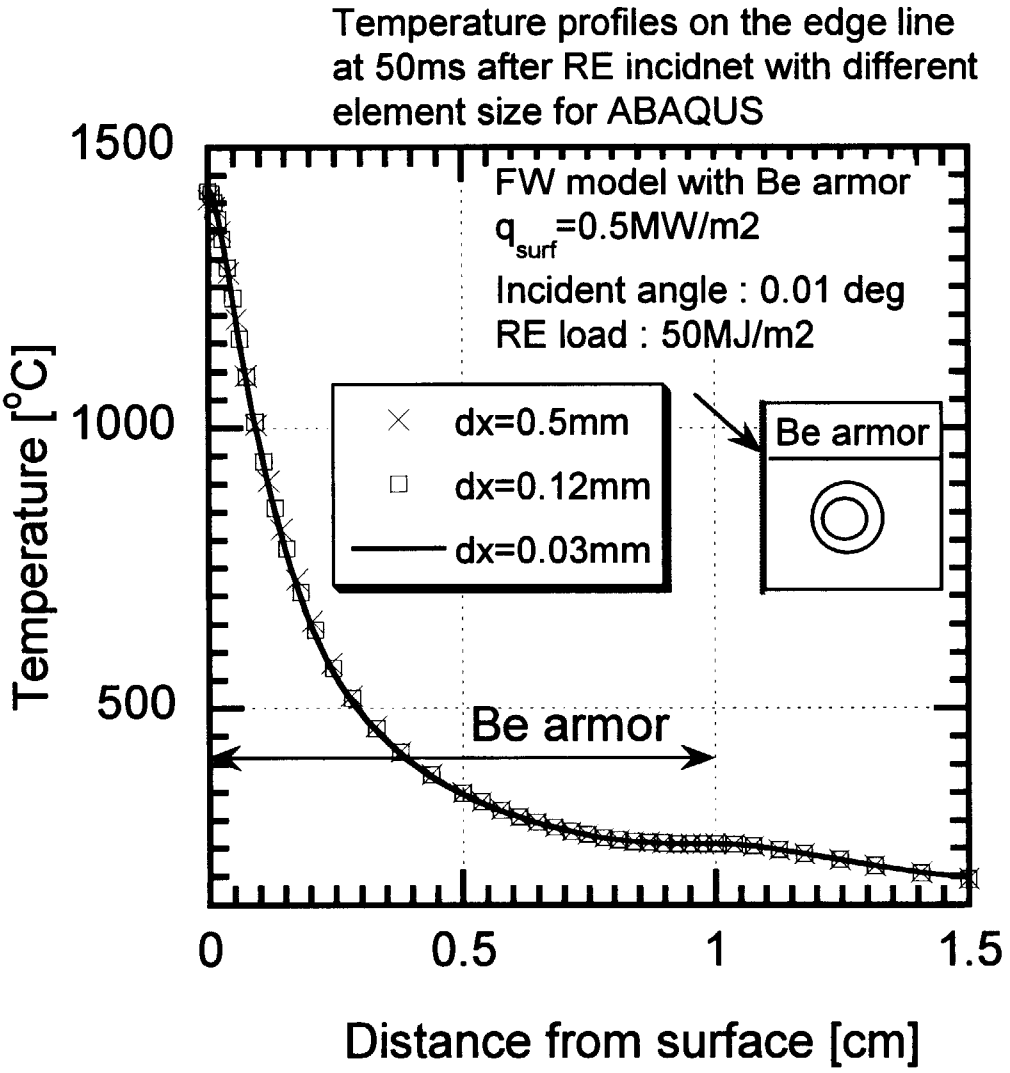

Figure A.3: Temperature profiles along edge line of FW model at 50 ms after start of runaway electrons impact from the results by using three element size of ABAQUS (I). Incident angle and magnetic field are 0.01 deg and 6 T. Surface heat flux of 0.5 MW/m^2 is taken into account for core plasma.

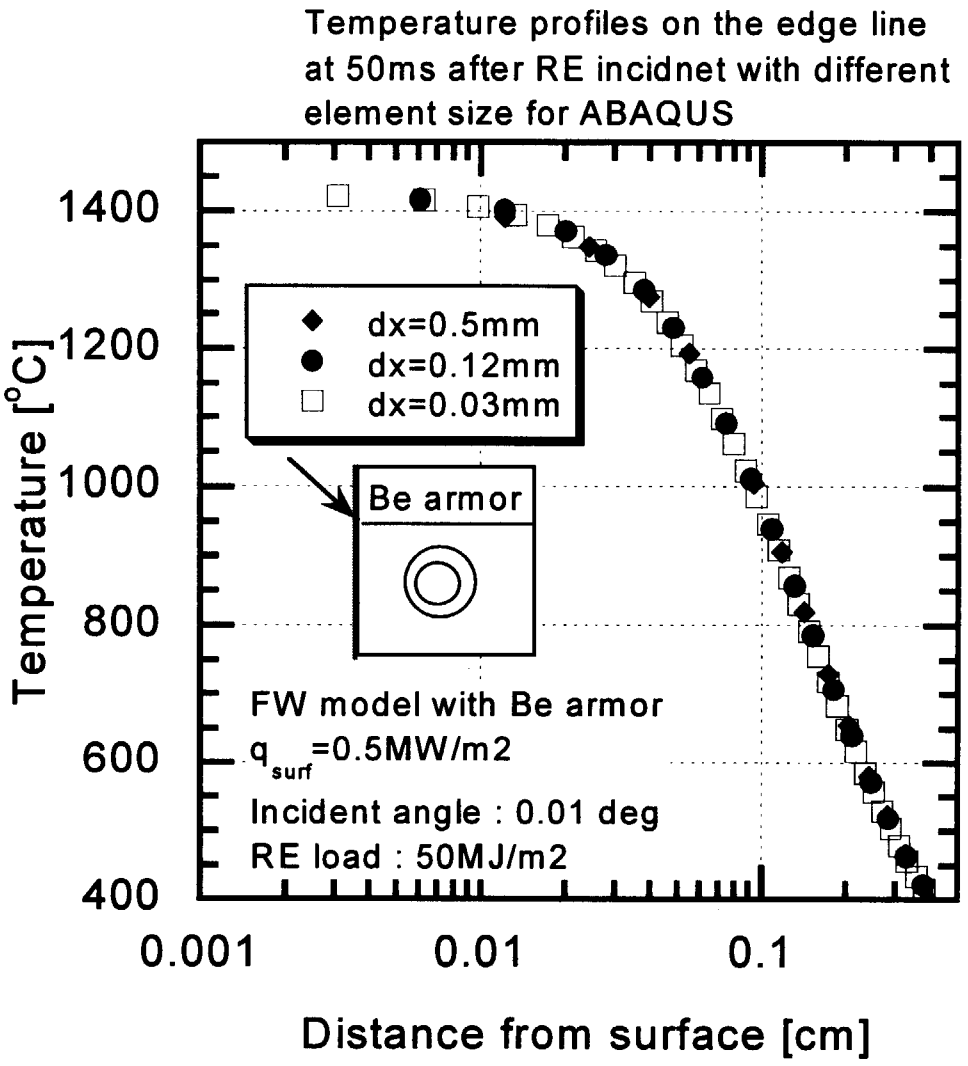

Figure A.4: Temperature profiles along edge line of FW model at 50 ms after start of runaway electrons impact from the results by using three element size of ABAQUS (II). Incident angle and magnetic field are 0.01 deg and 6 T. Surface heat flux of 0.5 MW/m^2 is taken into account for core plasma.

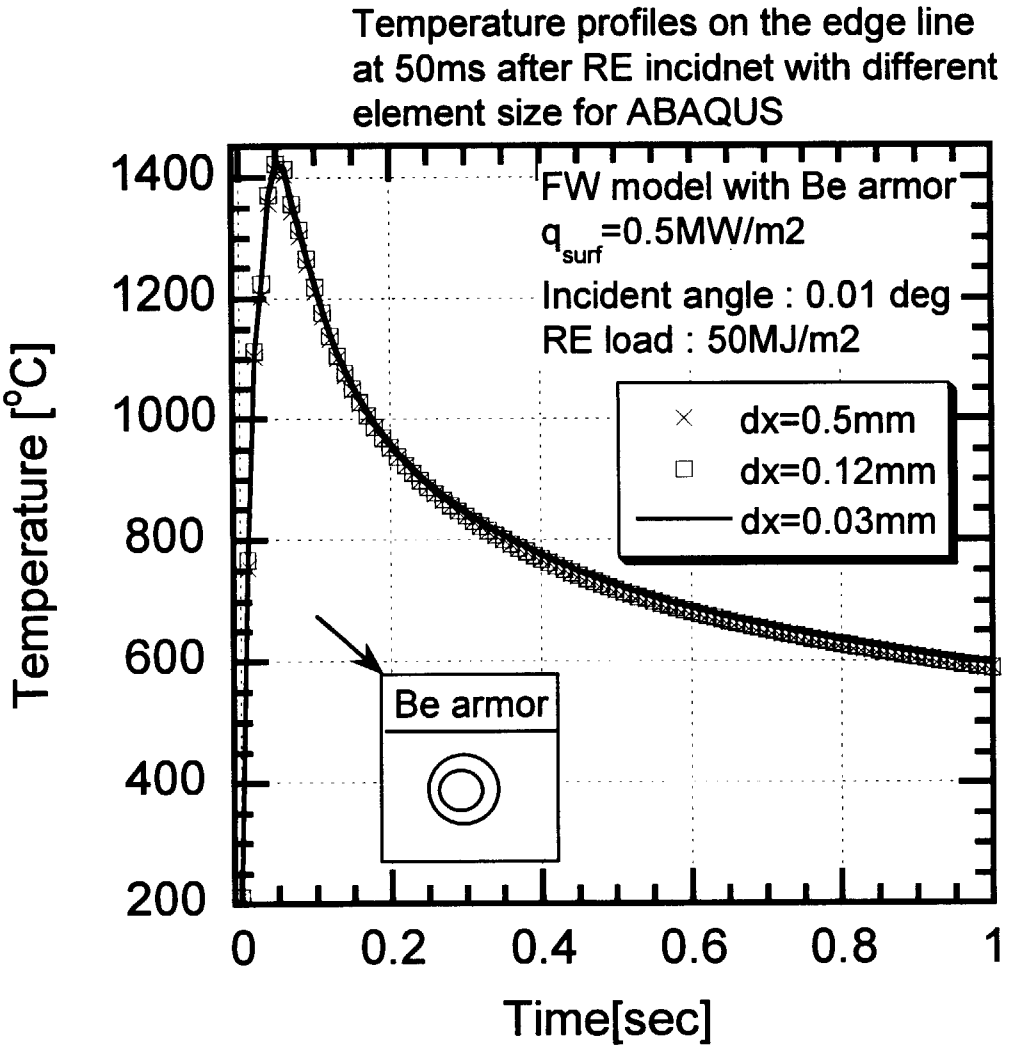

Figure A.5: Temperature profiles at the edge of FW surface at 50 ms after start of runaway electron impact from the results by using several element size of ABAQUS. Incident angle and magnetic field are 1 deg and 6 T. Surface heat flux of 0.5 MW/m^2 is taken into account for core plasma.

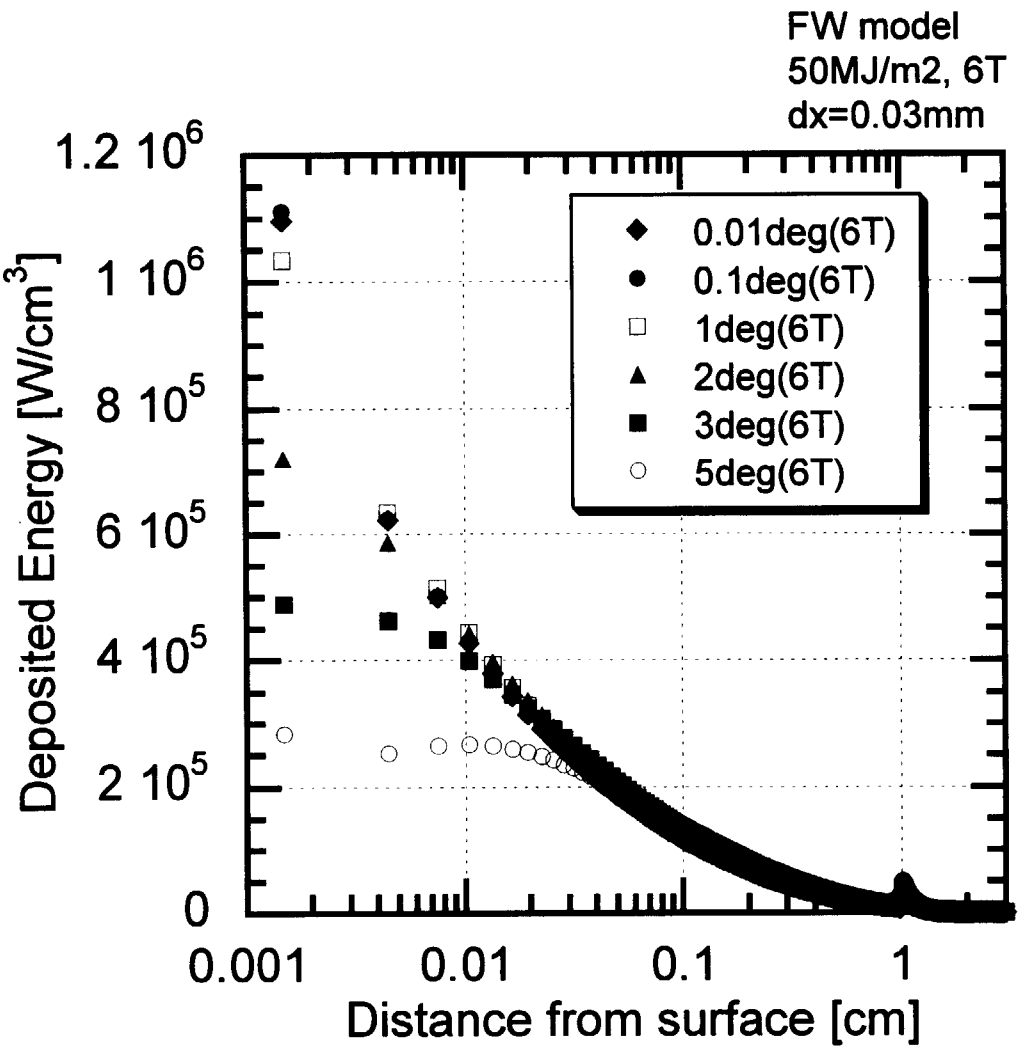

Figure A.6: Profiles of the heat generation in FW model at 50 ms after start of runaway electron impact from the results by using several incident angle of runaway electrons $\alpha = 0.01\,\mathrm{deg} - 5\,\mathrm{deg}$. Incident angle and magnetic field are 1 deg and 6 T.

This is a blank page.

国際単位系（SI）と換算表

表1　SI基本単位および補助単位

量	名称	記号
長さ	メートル	m
質量	キログラム	kg
時間	秒	s
電流	アンペア	A
熱力学温度	ケルビン	K
物質量	モル	mol
光度	カンデラ	cd
平面角	ラジアン	rad
立体角	ステラジアン	sr

表2　SIと併用される単位

名称	記号
分，時，日	min，h，d
度，分，秒	°，′，″
リットル	l，L
トン	t
電子ボルト	eV
原子質量単位	u

1 eV=1.60218×10^{-19}J

1 u=1.66054×10^{-27}kg

表3　固有の名称をもつSI組立単位

量	名称	記号	他のSI単位による表現
周波数	ヘルツ	Hz	s^{-1}
力	ニュートン	N	$m\cdot kg/s^2$
圧力，応力	パスカル	Pa	N/m^2
エネルギー，仕事，熱量	ジュール	J	N·m
工率，放射束	ワット	W	J/s
電気量，電荷	クーロン	C	A·s
電位，電圧，起電力	ボルト	V	W/A
静電容量	ファラド	F	C/V
電気抵抗	オーム	Ω	V/A
コンダクタンス	ジーメンス	S	A/V
磁束	ウェーバ	Wb	V·s
磁束密度	テスラ	T	Wb/m^2
インダクタンス	ヘンリー	H	Wb/A
セルシウス温度	セルシウス度	℃	
光束	ルーメン	lm	cd·sr
照度	ルクス	lx	lm/m^2
放射能	ベクレル	Bq	s^{-1}
吸収線量	グレイ	Gy	J/kg
線量等量	シーベルト	Sv	J/kg

表4　SIと共に暫定的に維持される単位

名称	記号
オングストローム	Å
バーン	b
バール	bar
ガル	Gal
キュリー	Ci
レントゲン	R
ラド	rad
レム	rem

1 Å=0.1nm=10^{-10}m

1 b=100fm^2=10^{-28}m^2

1 bar=0.1MPa=10^{5}Pa

1 Gal=1cm/s^2=10^{-2}m/s^2

1 Ci=3.7×10^{10}Bq

1 R=2.58×10^{-4}C/kg

1 rad=1cGy=10^{-2}Gy

1 rem=1cSv=10^{-2}Sv

表5　SI接頭語

倍数	接頭語	記号
10^{18}	エクサ	E
10^{15}	ペタ	P
10^{12}	テラ	T
10^{9}	ギガ	G
10^{6}	メガ	M
10^{3}	キロ	k
10^{2}	ヘクト	h
10^{1}	デカ	da
10^{-1}	デシ	d
10^{-2}	センチ	c
10^{-3}	ミリ	m
10^{-6}	マイクロ	μ
10^{-9}	ナノ	n
10^{-12}	ピコ	p
10^{-15}	フェムト	f
10^{-18}	アト	a

（注）

1．表1　5は「国際単位系」第5版，国際度量衡局1985年刊行による。ただし，1 eVおよび1 uの値はCODATAの1986年推奨値によった。

2．表4には海里，ノット，アール，ヘクタールも含まれているが日常の単位なのでここでは省略した。

3．barは，JISでは流体の圧力を表わす場合に限り表2のカテゴリーに分類されている。

4．EC閣僚理事会指令ではbar，barnおよび「血圧の単位」mmHgを表2のカテゴリーに入れている。

換算表

力	N(=10^{5}dyn)	kgf	lbf
	1	0.101972	0.224809
	9.80665	1	2.20462
	4.44822	0.453592	1

粘度　1 Pa·s(N·s/m^2)=10 P(ポアズ)(g/(cm·s))

動粘度　1m^2/s=10^{4}St(ストークス)(cm^2/s)

圧力	MPa(=10bar)	kgf/cm^2	atm	mmHg(Torr)	lbf/in^2(psi)
	1	10.1972	9.86923	7.50062×10^3	145.038
	0.0980665	1	0.967841	735.559	14.2233
	0.101325	1.03323	1	760	14.6959
	1.33322×10^{-4}	1.35951×10^{-3}	1.31579×10^{-3}	1	1.93368×10^{-2}
	6.89476×10^{-3}	7.03070×10^{-2}	6.80460×10^{-2}	51.7149	1

エネルギー・仕事・熱量	J(=10^7 erg)	kgf·m	kW·h	cal(計量法)	Btu	ft·lbf	eV
	1	0.101972	2.77778×10^{-7}	0.238889	9.47813×10^{-4}	0.737562	6.24150×10^{18}
	9.80665	1	2.72407×10^{-6}	2.34270	9.29487×10^{-3}	7.23301	6.12082×10^{19}
	3.6×10^6	3.67098×10^5	1	8.59999×10^5	3412.13	2.65522×10^6	2.24694×10^{25}
	4.18605	0.426858	1.16279×10^{-6}	1	3.96759×10^{-3}	3.08747	2.61272×10^{19}
	1055.06	107.586	2.93072×10^{-4}	252.042	1	778.172	6.58515×10^{21}
	1.35582	0.138255	3.76616×10^{-7}	0.323890	1.28506×10^{-3}	1	8.46233×10^{18}
	1.60218×10^{-19}	1.63377×10^{-20}	4.45050×10^{-26}	3.82743×10^{-20}	1.51857×10^{-22}	1.18171×10^{-19}	1

1 cal= 4.18605J（計量法）

= 4.184J（熱化学）

= 4.1855J（15℃）

= 4.1868J（国際蒸気表）

仕事率　1 PS(仏馬力)

= 75 kgf·m/s

= 735.499W

放射能	Bq	Ci
	1	2.70270×10^{-11}
	3.7×10^{10}	1

吸収線量	Gy	rad
	1	100
	0.01	1

照射線量	C/kg	R
	1	3876
	2.58×10^{-4}	1

線量当量	Sv	rem
	1	100
	0.01	1

（86年12月26日現在）

NUMERICAL SIMULATION OF RUNAWAY ELECTRON EFFECT ON PLASMA FACING COMPONENTS